HUMAN GENE THERAPY 23:635–646 (June 2012)

DOI: 10.1089/hum.2011.186

X-Linked Inhibitor of Apoptosis Protein-Mediated Attenuation of Apoptosis, Using a Novel Cardiac-Enhanced Adeno-Associated Viral Vector

Valentino Piacentino III,[1] Carmelo A. Milano,[1] Michael Bolanos,[1] Jacob Schroder,[1] Emily Messina,[1] Adam S. Cockrell,[2] Edward Jones,[1] Ava Krol,[3] Nenad Bursac,[3] Lan Mao,[4] Gayathri R. Devi,[5,6] R. Jude Samulski,[7] and Dawn E. Bowles[6]

Abstract

Successful amelioration of cardiac dysfunction and heart failure through gene therapy approaches will require a transgene effective at attenuating myocardial injury, and subsequent remodeling, using an efficient and safe delivery vehicle. Our laboratory has established a well-curated, high-quality repository of human myocardial tissues that we use as a discovery engine to identify putative therapeutic transgene targets, as well as to better understand the molecular basis of human heart failure. By using this rare resource we were able to examine age- and sex-matched left ventricular samples from (1) end-stage failing human hearts and (2) nonfailing human hearts and were able to identify the X-linked inhibitor of apoptosis protein (XIAP) as a novel target for treating cardiac dysfunction. We demonstrate that XIAP is diminished in failing human hearts, indicating that this potent inhibitor of apoptosis may be central in protecting the human heart from cellular injury culminating in heart failure. Efforts to ameliorate heart failure through delivery of XIAP compelled the design of a novel adeno-associated viral (AAV) vector, termed SASTG, that achieves highly efficient transduction in mouse heart and in cultured neonatal rat cardiomyocytes. Increased XIAP expression achieved with the SASTG vector inhibits caspase-3/7 activity in neonatal cardiomyocytes after induction of apoptosis through three common cardiac stresses: protein kinase C-γ inhibition, hypoxia, or β-adrenergic receptor agonist. These studies demonstrate the potential benefit of XIAP to correct heart failure after highly efficient delivery to the heart with the rationally designed SASTG AAV vector.

Introduction

Heart failure affects an estimated 5.7 million Americans, with approximately 300,000 deaths per year (Roger *et al.*, 2012a,b). The chronic and disabling nature of heart failure places an extreme economic burden on health care resources, and given the predicted increasing incidence of heart failure, the problem will only worsen. Gene therapy is a promising therapeutic option for heart failure (Williams and Koch, 2004; Whelan *et al.*, 2010; Pacak and Byrne, 2011; Wasala *et al.*, 2011). Ongoing clinical trials for the correction of cardiac diseases have demonstrated tolerability, safety, and biological effects, but further advances in gene therapy for heart failure are still required for its widespread use. Here we report on our efforts to identify and characterize a new molecular target for heart failure as well as our efforts to significantly improve adeno-associated viral (AAV) capsid design enabling more efficient cardiac gene delivery. Together, these two factors may enable more successful gene therapy for heart failure.

Many conditions may lead to heart failure. However, apoptosis or programmed cell death has been implicated as a common underlying, cellular process involved in many

[1]Cardiothoracic Division, Department of Surgery, Duke University Medical Center, Durham, NC 27710.
[2]Carolina Vaccine Institute, University of North Carolina at Chapel Hill, Chapel Hill, NC 27599.
[3]Department of Biomedical Engineering, Duke University, Durham, NC 27710.
[4]Division of Cardiology, Department of Medicine, Duke University Medical Center, Durham, NC 27710.
[5]Department of Pathology, Duke University Medical Center, Durham, NC 27710.
[6]Division of Surgical Sciences, Department of Surgery, Duke University Medical Center, Durham, NC 27710.
[7]Gene Therapy Center, University of North Carolina at Chapel Hill, Chapel Hill, NC 27599.

forms of human heart disease (Masri and Chandrashekhar, 2008). Much of the progressive deterioration of cardiomyocyte function during heart failure as well as cardiomyocyte damage during ischemia reperfusion is thought to occur because of apoptosis. In humans, it has been estimated that the apoptotic index in nonfailing human hearts is less than 0.5% whereas in heart disease or heart failure, it is increased 2- to 100-fold (Khoynezhad *et al.*, 2007). Interruption of the apoptotic pathway, either at the initial cardiac insult or during the progression of the disease, may have the potential to ameliorate many forms of cardiomyopathies. To date there has been a paucity of experimental attempts to modify the apoptotic cascade in models of heart disease, and this strategy has not been studied clinically (Laugwitz *et al.*, 2001; Chatterjee *et al.*, 2002; Okada *et al.*, 2005, 2009).

Cysteine-aspartic proteases, or caspases, the downstream effector molecules activated in apoptosis, trigger lethal events in both the cytoplasm and the nucleus (Czerski and Nunez, 2004; Regula and Kirshenbaum, 2005; Zorc-Pleskovic *et al.*, 2006; Gustafsson and Gottlieb, 2008; Masri and Chandrashekhar, 2008). Caspase-3, the terminal enzyme in this cascade, resides as a proenzyme until activated by upstream enzymes such as caspase-8, caspase-9, or granzyme. Caspase-3 levels, and activity, are regulated by a family of proteins termed inhibitors of apoptosis proteins (IAPs) (O'Riordan *et al.*, 2008). Although eight distinct human IAPs have been described in the literature (O'Riordan *et al.*, 2008), the X-linked inhibitor of apoptosis protein (XIAP) is considered the most potent as it directly inhibits the enzymatic activities of not only caspase-3 but also of caspases 7 and 9 (O'Riordan *et al.*, 2008). In addition, XIAP contains E3 ubiquitin ligase activity, which can promote the ubiquitination of caspase-3, further decreasing caspase-3 activity (O'Riordan *et al.*, 2008).

Here, we demonstrate that XIAP expression is diminished in failing human hearts compared with nonfailing controls. Therefore, a goal of this study was to mitigate putative apoptotic effects through efficient delivery, and expression, of XIAP. The ideal vector for this study would minimally impact the apoptosis cascade, provide high-level, long-term gene expression, and be safe for eventual clinical use. Adeno-associated viral (AAV) vectors meet many of these requirements and are rapidly becoming vectors used in clinical trials for cardiovascular gene delivery (Hajjar *et al.*, 2008; Jaski *et al.*, 2009; Gwathmey *et al.*, 2011). Ongoing in the AAV field is the identification of AAV serotypes or the development of AAV capsid variants that render high-level transduction in target organs such as skeletal and cardiac muscle (Du *et al.*, 2004; Wang *et al.*, 2005; Su *et al.*, 2006, 2008; Palomeque *et al.*, 2007; Bish *et al.*, 2008a,b; Zincarelli *et al.*, 2008; Tarantal and Lee, 2009; Yang *et al.*, 2009; Pulicherla *et al.*, 2011). Previously, by using a rational design approach we were able to identify five amino acids of the AAV1 capsid as responsible for efficient skeletal muscle transduction (Bowles *et al.*, 2011). Here we have evaluated the influence of these five amino acids, engineered individually and in groups in the context of both the AAV2 and AAV3b capsids, on the transduction of murine skeletal and cardiac muscle. The modification of two of these amino acids in the AAV3b capsid rendered a capsid exhibiting extremely high-level cardiac muscle transduction. Using this novel AAV3b vector, termed SASTG, to deliver the XIAP gene into rat neonatal cardiomyocytes, we demonstrate that this potent apoptotic inhibitor attenuates apoptosis induced by protein kinase C (PKC) inhibition, hypoxia/ischemia, or isoproterenol stimulation. These studies demonstrate the development of an innovative AAV vector (SASTG) for efficient delivery of a novel antiapoptotic transgene (XIAP) with potential cardioprotective impact during human heart failure.

Materials and Methods

Human myocardium acquisition

Human myocardium was obtained from unused "nonfailing" donor hearts and explanted hearts from cardiac transplantation. All hearts were arrested *in vivo*, with cardioplegia (4°C). Anterolateral samples of the left ventricle were then obtained and snap frozen in liquid nitrogen. The study was approved by the Institutional Review Board at Duke University Medical Center (Durham, NC).

Protein isolation and XIAP immunodetection

Left ventricular samples were placed in homogenization buffer and homogenized while on ice. The homogenate was centrifuged and the supernatant was used for study. All protein homogenates were subjected to bicinchoninic acid (BCA) assay (Pierce Biotechnology/Thermo Fisher Scientific, Rockford, IL) for protein quantification. XIAP present in the human myocardial lysate was quantified by Western blotting. Protein samples (75 μg per lane) were electrophoresed on a 10–20% Tris–glycine gel (Invitrogen, Carlsbad, CA), transferred to a nitrocellulose membrane, and probed with a 1:500 dilution of mouse anti-XIAP antibody (BD Biosciences, San Jose, CA) followed by a 1:2500 dilution of enhanced chemiluminescence (ECL) anti-mouse IgG horseradish peroxidase-linked antibody (GE Healthcare Bio-Sciences, Piscataway, NJ), and detected with detection reagent (GE Healthcare Bio-Sciences). Nitrocellulose blots were stripped and reprobed with a 1:500 diluted monoclonal anti-sarcomeric actin antibody (Sigma-Aldrich, St. Louis, MO). XIAP and actin signals were quantified with ImageJ (National Institutes of Health [NIH], Bethesda, MD) and XIAP expression levels were normalized to actin. XIAP levels were also quantified with a Proteome Profiler human apoptosis array kit as per the manufacturer's instructions (R&D Systems, Minneapolis, MN). XIAP was quantified in duplicate from each homogenate. Data are represented as raw optical units (ROU).

Plasmid and DNA mutagenesis

Starting plasmids for mutagenesis were the packaging plasmids pXR2 and pXR3 (Rabinowitz *et al.*, 2002). All plasmid mutagenesis was performed with either a QuikChange multi site-directed mutagenesis or QuikChange site-directed mutagenesis kit (both from Stratagene/Agilent Technologies, Santa Clara, CA). Accuracy of the nucleotide changes was verified by DNA sequence analyses followed by DNA subcloning to eliminate any unwanted artifacts generated by the mutagenesis.

AAV vector development and production

The plasmid carrying the cDNA for human X-linked inhibitor of apoptosis (XIAP) was obtained from the American

Type Culture Collection (ATCC, Manassas, VA). The XIAP cDNA was excised from the ATCC shuttle plasmid, using *Age*I and *Not*I digestion, and then ligated into the pTR vector. Recombinant XIAP-AAV, GFP-AAV, and Luciferase-AAV vectors were generated by the standard triple transfection method (reviewed in Grieger *et al.*, 2006), using the XX6-80 adenoviral helper plasmid with packaging plasmid (pXR1-9, Q263AT265, Q263A, T265, N705AV708AT716N, SASTG, or 3.1) and the TR plasmid carrying human XIAP, green fluorescent protein (GFP) (pTRUFr; Zolotukhin *et al.*, 1999), or firefly luciferase transgenes. rAAV-XIAP, rAAV-luciferase, and rAAV-GFP were purified by standard methodology (reviewed in Grieger *et al.*, 2006) and the physical titer was evaluated by dot-blot hybridization (reviewed in Grieger *et al.*, 2006). The adenoviral luciferase vector was obtained from the Pittsburgh Human Gene Therapy Center (Pittsburgh, PA).

Animals

C57BL and BALB/c mice were purchased from Jackson Laboratory (Bar Harbor, ME). Animals were maintained and treated in accordance with the Animal Care and Use Committee of the University of North Carolina at Chapel Hill (Chapel Hill, NC) (for skeletal muscle injections) or with the Animal Care and Use Committee at Duke University (for myocardial injections). All care and procedures were in accordance with the Guide for the Care and Use of Laboratory Animals (DHHS Publication No. [NIH] 85-23), and all procedures received prior approval by either the University of North Carolina or Duke University (Durham, NC) Institutional Animal Care and Use Committee.

Skeletal muscle injections

A volume containing 1×10^{10} viral genome-containing particles (VG) was injected into the gastrocnemius of male BALB/c mice (6 to 8 weeks old). A total of six limbs per experiment were injected for each vector type, using 25 μl of virus. The mice were anesthetized by intraperitoneal administration of 2.5% tribromoethanol (Avertin). A solution of the luciferase substrate luciferin (150 mg/kg; Invitrogen) was injected intraperitoneally. A gray-scale reference image of animals was generated and mice were imaged for 5 min, using a NightOWL cabinet with charge-coupled device (CCD) camera (Berthold Technologies, Bad Wildbad, Germany). Total photon emission from selected and defined areas within the images of each mouse was quantified with WinLight 32 software (Berthold Technologies). The photon signal was presented as a pseudo-color image representing light intensity. This image was superimposed on the reference image for orientation.

Direct myocardial injections

Four mice per vector type for each experiment were subjected to myocardial injection with 2×10^{10} VG. To perform the injections, mice were first anesthetized (a cocktail of ketamine [100 mg/kg] and xylazine [2.5 mg/kg]) and intubated (a blunt 20-gauge plastic needle connected to a rodent ventilator at a tidal volume of 0.2 ml and a respiratory rate of 105 breaths/min). The chest cavity was entered via the third intercostal space, with exposure of the left ventricle. Five to 10 μl of vector was injected into the anterior free wall of the left ventricle. After the injection, the chest was closed; pneumothorax was evacuated with a modified chest tube made of PE-50 polyethylene with multiple distal side-holes. The mice were extubated and allowed to recover from anesthesia. For imaging experiments, mice were anesthetized with isoflurane. One hundred microliters of luciferin was delivered via intraperitoneal injection, and animals were imaged 10 min after injection, using a Xenogen IVIS imaging system (Caliper Life Sciences/PerkinElmer, Hopkinton, MA) and luminescence was measured. Data are presented as relative light units per region of interest (ROI).

Rat neonatal cardiomyocyte isolation

Neonatal rat cardiomyocytes were isolated from ventricles of 2-day-old Sprague-Dawley rats (Charles River Laboratories, Wilmington, MA). Briefly, excised ventricles were minced and incubated overnight in a 0.07% solution of trypsin (Sigma-Aldrich) at 4°C, followed by four-step dissociation in 0.1% collagenase II (Worthington Biochemical, Lakewood, NJ) at 37°C (Pedrotty *et al.*, 2009). Dissociated cells were resuspended in culture medium (DMEM–F12 medium [Invitrogen] supplemented with 10% calf serum [Colorado Serum Company, Denver, CO] and 10% horse serum [HyClone/Thermo Fisher Scientific, Logan, UT]) and preplated in two 1-hr steps to remove faster adhering nonmyocytes (Pedrotty *et al.*, 2009).

Viral vector infections and experimental design

Neonatal cardiomyocytes plated at 10,000 cells per well were placed in cardiac medium containing 2% fetal bovine serum (FBS) 12 hr before infection with Ad-luciferase, SASTG-luciferase, SASTG-GFP, or SASTG-XIAP. All pharmacological treatments were performed on cells approximately 72 hr postinfection. All pharmacological treatments, including vehicle controls, were done in duplicate or triplicate. To induce apoptosis pharmacologically, chelerythrine (Yamamoto *et al.*, 2001) was added to the medium for 1 hr at a final concentration of 1 μM. This dose has previously been shown to induce caspase-3 activation and morphological cellular changes indicative of apoptosis (Yamamoto *et al.*, 2001). For isoproterenol experiments, isoproterenol (1 μM) was added to the media for 24 hr. For hypoxia–ischemia experiments, two 6-well dishes were incubated inside an airtight container at 37°C. Cardiomyocytes were placed in standard medium in a 95% O_2–5% CO_2 environment for 6 hr. The cells were then placed in medium with the following composition: 118 mM NaCl, 24 mM $NaHCO_3$, 1 mM NaH_2PO_4, 2.5 mM $CaCl_2$, 1.2 mM $MgCl_2$, 2 mM sodium-L-lactate, 16 mM KCl, and 10 mM 2-deoxyglucose and the chamber was superfused with 1% O_2, 5% CO_2, and 94% nitrogen for 12 hr. The gas was then switched back to 95% O_2–5% CO_2 for reoxygenation and the medium was switched to Medium 199 containing 2% FBS to reinstitute nutrients for 6 hr. Cells from all experiments were lysed and assayed for total protein (BCA assay) before assaying for caspase-3/7 activity.

Caspase-3/7 assay and firefly luciferase assay

Caspase-3/7 activity was measured with a Caspase-Glo 3/7 assay system (Promega, Madison, WI). Fifteen to 20 μg of

human heart lysate or rat neonatal cardiomyocyte lysate was added to a 96-well plate in the presence of the luminescent substrate. Luminescence was measured every 15 min during the 90-min observation period, using a Veritas luminometer from Turner BioSystems (Sunnyvale, CA). The signal was normalized to the protein loaded into each well. The appropriate positive and negative controls were performed to ensure that the majority of signal was from the lysates. Firefly luciferase activity was measured with luciferase assay reagent (Promega). Within the luminometer, wells were injected with 100 μl of luciferase assay reagent, and after a delay of 2 sec, a measurement was taken for 10 sec.

Statistics

Data are expressed as means followed by the standard deviation. Normalized immunoblot and caspase-3/7 assay data were compared by unpaired Student t test. A p value less than 0.05 was considered statistically significant.

Results

Enhanced apoptosis in failing human hearts is correlated with downregulation of XIAP, an inhibitor of apoptosis

Loss of apoptotic regulation may contribute to cell death leading to heart failure. Using tissue samples from a unique repository of failing and nonfailing human hearts (established by the authors in the Department of Surgery at Duke University), relative levels of protein markers of apoptosis were investigated. Because XIAP is a central modulator of apoptosis, we hypothesized that deregulation of XIAP may be a contributing factor in human heart failure. Protein analysis of XIAP in failing human myocardium, compared with nonfailing hearts, was assessed by two different assays. Quantitation of protein levels by Western blot analysis demonstrated a 38% decrease in XIAP expression in failing human myocardium, compared with nonfailing controls (Fig. 1A). In a complementary proteomics-based approach, antibody arrays also confirmed the presence of a significant loss of XIAP in failing hearts from four different individuals, compared with nonfailing control hearts from four distinct individuals (Fig. 1B and C). A statistically significant 33% decrease in XIAP was shown in failing human myocardium, using protein array technology (Fig. 1B and C). Importantly, caspase-3/7 activity was inversely related to XIAP expression, wherein caspase-3/7 activity increased by 267% in failing myocardium (Fig. 1D). Loss of XIAP expression may result in enhanced caspase-3/7 activity, and consequently increased cell death in failing human myocardium. Therefore, commissioning therapeutic gene delivery approaches to reconstitute XIAP expression in diseased human hearts may mitigate cell death associated with apoptosis.

Development of an AAV3b-derived vector, SASTG, that renders high-level cardiac tissue and cardiomyocyte transduction

AAV-derived vectors are amenable to rational design based on a combination of capsid structure predictions, sequence alignments, susceptibility to neutralizing antibodies, and distinct functional capabilities (Bowles *et al.*, 2011). The diminished capacity of AAV2 and AAV3b to transduce skeletal muscle make them amenable to gain-of-function studies to test rationally designed capsid variants, as demonstrated by the generation of AAV2.5 (Bowles *et al.*, 2011). Five amino acids (N705/V708/T716/Q263/T265), unique to AAV1, endow AAV2 with the capacity to transduce mouse skeletal muscle with greater efficiency than conventional AAV2, approaching that of AAV1 (Bowles *et al.*, 2011). Understanding that these five capsid amino acids dramatically influence AAV vector biology, we wanted to further

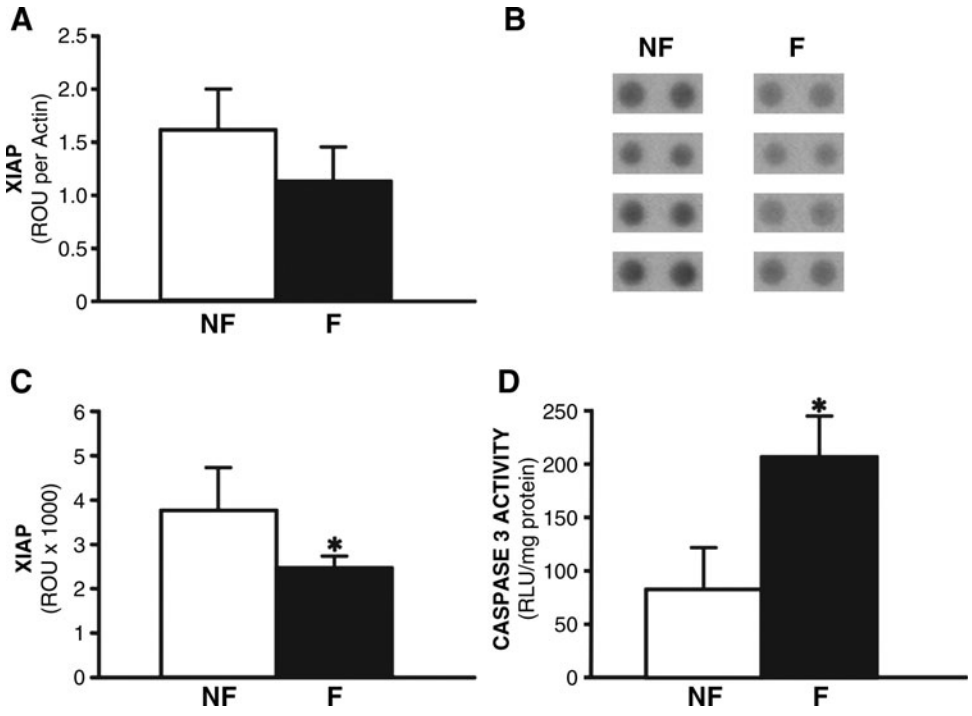

FIG. 1. X-linked inhibitor of apoptosis protein (XIAP) levels and caspase-3/7 activity in human heart failure. **(A)** Quantitation of XIAP Western blot as determined by densitometry analysis and expressed as raw optical units (ROU) normalized to actin levels. **(B)** Antibody array approach showing XIAP levels from four nonfailing (NF) and four failing (F) human hearts. Duplicate spots are presented for each heart. **(C)** Quantitation of antibody arrays by densitometry analysis, and expressed as raw optical units. **(D)** Caspase-3/7 activity in lysates from human nonfailing LV myocardium (NF) or failing human myocardium (F), and expressed as relative light units normalized for total protein. Bars represent the standard deviation; $*p < 0.05$.

investigate the biology of these capsid regions: (1) to assess the contribution of individual amino acids to the efficiency of AAV2 vector transduction and (2) to determine whether the enhanced transduction imparted by these amino acids is restricted to AAV2 or is part of a general transduction mechanism that can be extended to other serotypes such as AAV3b.

To investigate whether all five amino acids engineered into AAV2.5 were necessary for its enhanced skeletal muscle transduction two subvariants were generated, Q263A/T265 and N705A/V708A/T716N, and quantitated by *in vivo* imaging (Fig. 2A). Except for T265 (an insertion), all amino acid mutations were individual substitutions. Amino acid groupings were derived from the structural assessment of AAV2.5 (depicted in Bowles *et al.*, 2011; see Fig. 1C therein). Briefly, two capsid subunits meet at the 2-fold axis of symmetry where these five amino acids are in close proximity with the N705A/V708A/T716N grouping on one side of the axis and the Q263A/T265 grouping on the other. Figure 2A demonstrates that the N705A/V708A/T716N subvariant exhibited an inefficient skeletal muscle transduction profile, similar in efficiency to the AAV2 vector (Bowles *et al.*, 2011), whereas the Q263A/T265 subvariant was up to 9.8-fold more efficient. Further partitioning of the Q263A/T265 subvariant into AAV2 capsids with individual modifications, Q263A and T265, revealed that only the one amino acid insertion, T265, can confer on AAV2 the ability to transduce skeletal muscle with enhanced efficiency (Fig. 2B). Thus, the enhanced skeletal muscle transduction observed for AAV2.5 can be attributed primarily to the T265 insertion.

The rational identification of a portable capsid system that can augment the muscular transduction profile of various AAV serotypes may expand the availability of gene delivery vehicles, and provide insight into specific AAV capsid regions critical for transduction. Thus, the AAV3b capsid was modified to resemble the AAV2 Q263A/T265 subvariant by introducing these modifications at similar positions in the AAV3b capsid, and termed SASTG to distinguish it from conventional AAV3b. *In vivo* administration of SASTG to skeletal muscle was quantitated by luciferase expression at various times posttransduction (Fig. 2C). Intriguingly, SASTG exhibited significantly enhanced skeletal muscle transduction compared with conventional AAV3b, achieving skeletal muscle transduction levels similar to AAV1 (Fig. 2C). Further partitioning of SASTG to the single T265 insertion, AAV3.1, did not reach SASTG transduction levels in skeletal muscle (Fig. 2D). These results indicate that the Q263A/T265 subvariant group is necessary to fully augment transduction of skeletal muscle for AAV3b (SASTG vector), whereas only the T265 mutation was necessary for AAV2.

In skeletal muscle SASTG and the T265 AAV2 subvariants achieved transduction efficiencies that approach those of

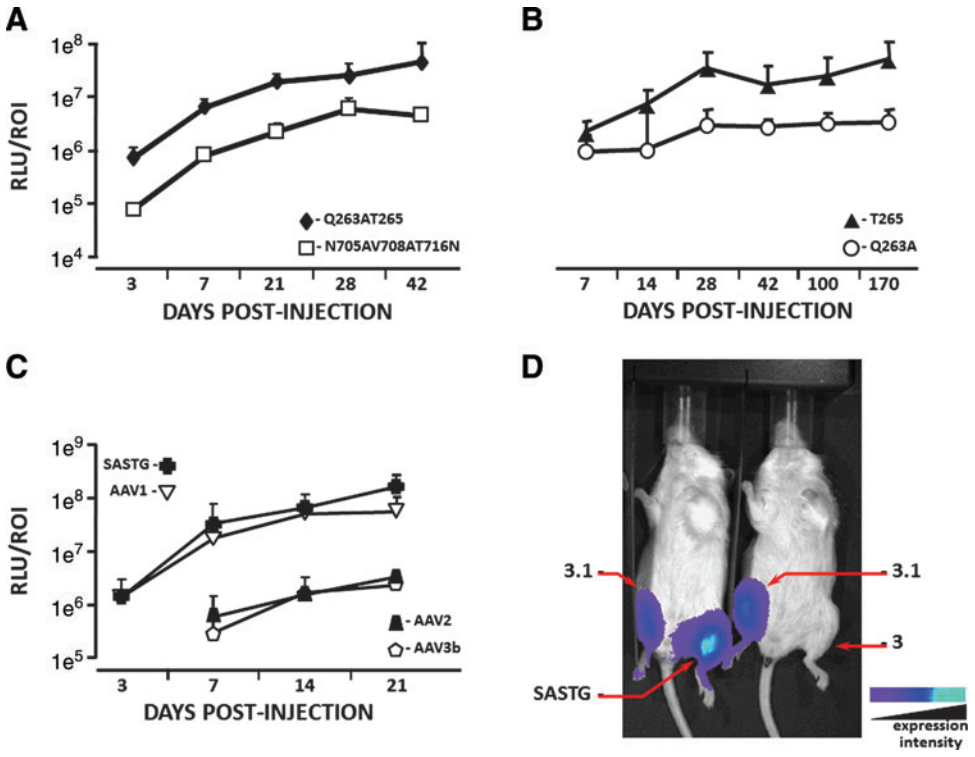

FIG. 2. Evaluation of skeletal muscle transduction by AAV variants, using biophotonic imaging. Skeletal muscle transduction of **(A)** Q263AT265-luciferase and N705AV708AT716N-luciferase vectors was examined on days 3, 7, 21, 28, and 42 postinjection. **(B)** Q263A-luciferase and T265-luciferase vectors were examined on days 7, 14, 28, 42, 100, and 170 postinjection. **(C)** AAV1-, AAV2-, AAV3b-, and SASTG-luciferase vectors were examined on days 3, 7, 14, and 21. For each experiment in **(A)**, **(B)**, and **(C)** each limb ($n=6$ limbs per group) was injected with 1×10^9 genome particles in each gastrocnemius muscle. Data are expressed as relative light units per region of interest (RLU/ROI). **(D)** Comparison of skeletal muscle transduction of AAV3, AAV3.1, and SASTG, using *in vivo* biophotonic imaging of hind leg injections. Increasing wavelength reflects greater luminescence. Color images available online at www.liebertonline.com/hum

AAV1. In rodent heart muscle AAV1, the closely related AAV6 serotype, and AAV9 have been reported to mediate higher levels of gene expression than AAV2 (Kawamoto *et al.*, 2005; Pacak *et al.*, 2006; Su *et al.*, 2006; Palomeque *et al.*, 2007). Studies comparing AAV6, AAV8, and AAV9 in nonhuman primates indicate that AAV6 achieves the most efficient, widespread, and most cardiac-specific gene expression in this model (Gao *et al.*, 2011). To investigate the potential that the T265 AAV2 subvariant and SASTG may acquire a cardiac muscle transduction profile similar to AAV1, AAV6, or AAV9, vectors were directly administered to rodent hearts, and transduction profiles were quantitated over time by luciferase expression (Fig. 3). Both AAV2 subvariants (Q263A/T265 and T265) exhibited greatly enhanced cardiac muscle transduction, compared with conventional AAV2 (Fig. 3A). Surprisingly, SASTG attained transduction efficiencies that were up to 21-fold greater than AAV1 (Fig. 3B). Compared with AAV9, which also exhibits efficient cardiac transduction (Pacak *et al.*, 2006), SASTG was greater than 8-fold more efficient at cardiac muscle transduction in two independent experiments (Fig. 3C and D). Importantly, when compared with AAV9, expression arising from SASTG appears to remain localized in the heart (Fig. 3C), whereas expression arising from AAV9 appears to spread from the initial site of injection to other organs, such as the liver (Fig. 3C). In addition, the SASTG vector appears to achieve substantial expression by day 2 compared with the AAV9 vector (Fig. 3D). Overall, SASTG exhibits more efficient transduction than AAV1 or AAV9 on *in vivo* administration to cardiac tissue.

These studies were extended to test the transduction capacity of SASTG against a panel of AAV-luciferase vectors representing conventional AAV serotypes 1–9. Rat neonatal cardiomyocytes can be routinely isolated in our laboratory to investigate cardiac function at the molecular and cellular levels. To assess whether SASTG offered higher transduction levels than other AAV serotypes, cardiomyocytes were transduced with an equivalent number of genomes from each AAV-luciferase vector. Of the serotypes tested, only AAV1, AAV6, and SASTG rendered substantial increases in luciferase expression (Fig. 4). In accordance with the *in vivo* mouse imaging analysis, SASTG achieved the highest expression levels, which were 26-fold greater than AAV1 and 61-fold greater than AAV6 (Fig. 4). Clearly, SASTG would be highly desirable for therapeutic transgene delivery to cardiac tissue *in vivo*, as well as *in vitro*. Cardiac tissue delivery of XIAP with the AAV3b-derived SASTG vector may alleviate apoptotic effects that contribute to heart failure.

Delivery of XIAP by SASTG vector ameliorates apoptosis in rat neonatal cardiomyocytes

Some cardiomyopathies are associated with naturally occurring viral infections such as adenovirus (Savon *et al.*, 2008). Apoptosis induced by these viral infections may contribute to rapidly developing cardiomyopathies. Anticipating the use of the SASTG AAV-derived vector to deliver XIAP to mitigate apoptotic effects in failing hearts, it was prudent to evaluate the capacity of the SASTG vector to

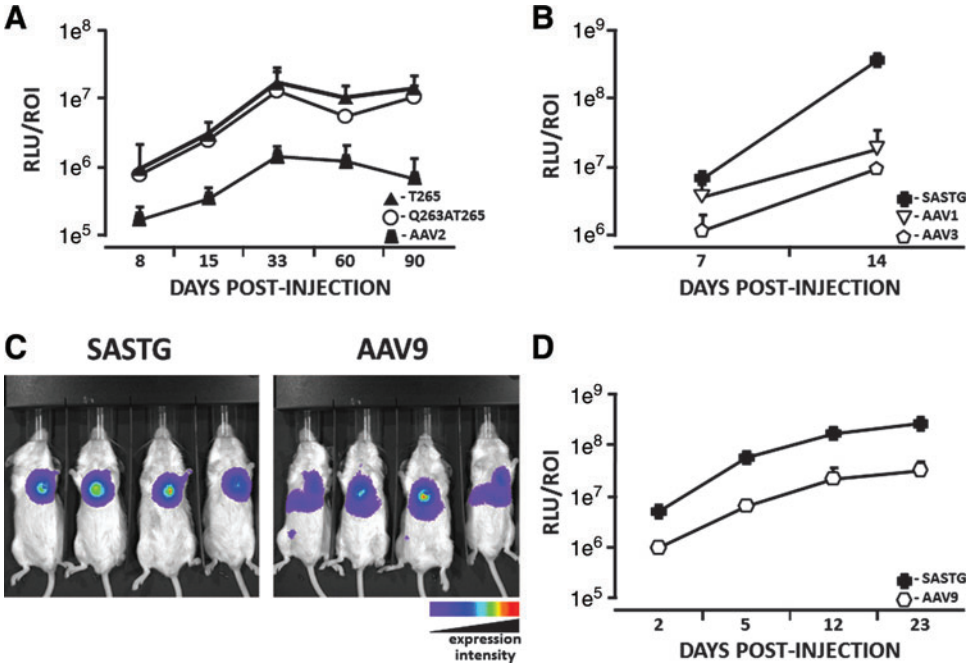

FIG. 3. Evaluation of cardiac muscle transduction by AAV variants, using *in vivo* biophotonic imaging. **(A)** Cardiac muscle transduction by AAV2-, T265-, and Q263AT265-luciferase vectors was examined on days 8, 15, 33, 60, and 90 postinjection. **(B)** Cardiac muscle transduction by AAV1-, AAV3- and SASTG-luciferase vectors was examined on days 7 and 14 postinjection. **(C)** Image showing *in vivo* expression of SASTG and AAV9 23 days after direct cardiac injection. Increasing wavelength reflects greater luminescence. **(D)** Quantification of *in vivo* biophotonic imaging time course (days 2, 5, 12, 23), comparing luciferase expression of AAV9 and SASTG injected directly into mouse myocardium. For each experiment: $n=4$ mice per group and 2×10^9 genome particles of each vector was injected directly into the myocardium of each mouse. Data are expressed as relative light units per region of interest (RLU/ROI). Color images available online at www.liebertonline.com/hum

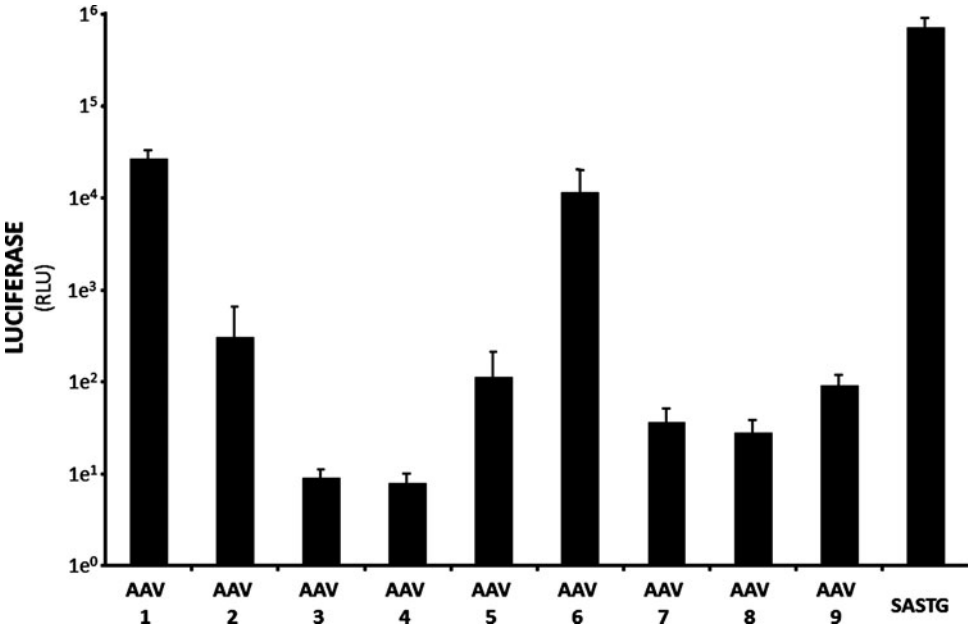

FIG. 4. Efficiency of SASTG transduction in rat neonatal cardiomyocytes (RNNCs). Freshly isolated RNNCs were transduced with AAV1-9 and SASTG at 50,000 particles per cell, all bearing the luciferase transgene. The vectors were applied to 10,000 cells in a 96-well format. Light emitted from the infections was assayed by luminometry the next day. These experiments in RNNCs were repeated a total of three times and data similar to those shown in Fig. 4 were observed each time. Data represent means and SD.

activate apoptosis in cardiomyocytes. Therefore, SASTG-luciferase was compared with adenovirus-luciferase vectors for their capacity to induce apoptosis in rat neonatal cardiomyocytes (Fig. 5). SASTG and adenoviral vectors were assessed for transduction by measuring luciferase activity 24, 48, and 72 hr postinfection, using 100 particles/cell for adenovirus and 50,000 particles/cell for SASTG. Empirical studies demonstrated that these were optimal doses to achieve equivalent transduction efficiencies over time, as demonstrated in Fig. 5A. Concomitantly, caspase-3/7 activity was assessed as a measure of apoptosis (Fig. 5B). Transduction with SASTG vector induced substantially lower levels of caspase-3/7 at all times, compared with adenoviral vector (Fig. 5B). Most importantly, at the 72-hr time point when SASTG and the adenoviral vector exhibited approximate equal transgene expression (Fig. 5A), caspase-3/7 activity associated with the SASTG infection was 11.5-fold lower than that observed with adenoviral transduction; a distinction made obvious by the ratio of transduction relative to caspase-3/7 activity (Fig. 5C). The nearly absent levels of induced apoptosis combined with high transduction efficiency make SASTG a suitable vehicle to deliver a transgene that can interfere with apoptosis.

The aforementioned data suggest that XIAP may be a therapeutic target for modulating apoptosis in heart failure. The XIAP transgene was incorporated into the highly efficient SASTG capsid and examined for the ability to attenuate apoptosis *in vitro.* To determine whether increased expression of XIAP was protective, neonatal cardiomyocytes were cultured and transduced with SASTG-XIAP, and compared with SASTG-GFP as a control. Apoptosis was subsequently induced by treatment of the cells with the protein kinase C (PKC)-γ inhibitor chelerythrine. Chelerythrine has been shown to activate apoptosis through the intrinsic pathway, resulting in cleavage of procaspase-3 (Yamamoto *et al.*, 2001). Figure 6 shows representative light microscopy photographs of chelerythrine-exposed cardiomyocytes that had been pretreated with SASTG-GFP (Fig. 6, left) or SASTG-XIAP (Fig. 6, right). Note the paucity of cytoplasm and condensation of the nuclei of the cardiomyocytes treated with SASTG-GFP. In contrast, cardiomyocytes overexpressing XIAP demonstrated robust cytoplasm volume with no obvious condensation of the nuclei when exposed to chelerythrine. These data indicate that apoptosis could be effectively induced in cardiomyocytes in the absence of XIAP protection.

The protective nature of XIAP in cardiomyocytes was further assessed by measuring caspase-3/7 activity after induction of apoptosis by three different cardiac stresses. In accordance with data in Fig. 6, significantly less caspase-3/7 activity was observed after chelerythrine (CHEL) exposure in cells expressing XIAP relative to cells transduced with SASTG-GFP vector (Fig. 7). These data suggest that expression of XIAP attenuates apoptosis induced by PKC-γ inhibition. We also studied the effects of XIAP on β-adrenergically induced apoptosis, given that this signaling pathway is believed to be the major inducer of apoptosis during heart failure. Cardiomyocytes pretreated with SASTG-XIAP were protected against caspase-3/7 activation after stimulation with isoproterenol (ISO), compared with SASTG-GFP control vector (Fig. 7). A third stress commonly encountered in heart failure patients is hypoxia–ischemia (H/I). Apoptosis in neonatal cardiomyocytes was induced by exposure to a hypoxic environment followed by reexposure to normal medium and oxygen tension. Optimal conditions that induce apoptosis were empirically determined. Similar to other stresses, cardiomyocytes treated with SASTG-XIAP exhibited significantly less caspase-3/7 activation compared with SASTG-GFP control (Fig. 7). These data clearly demonstrate that XIAP can ameliorate apoptosis induced in cardiomyocytes by stresses associated with heart failure.

Discussion

Heart failure, the inability of the heart to pump sufficient blood to meet the metabolic demands of the body, is an important health problem in this country and worldwide. At

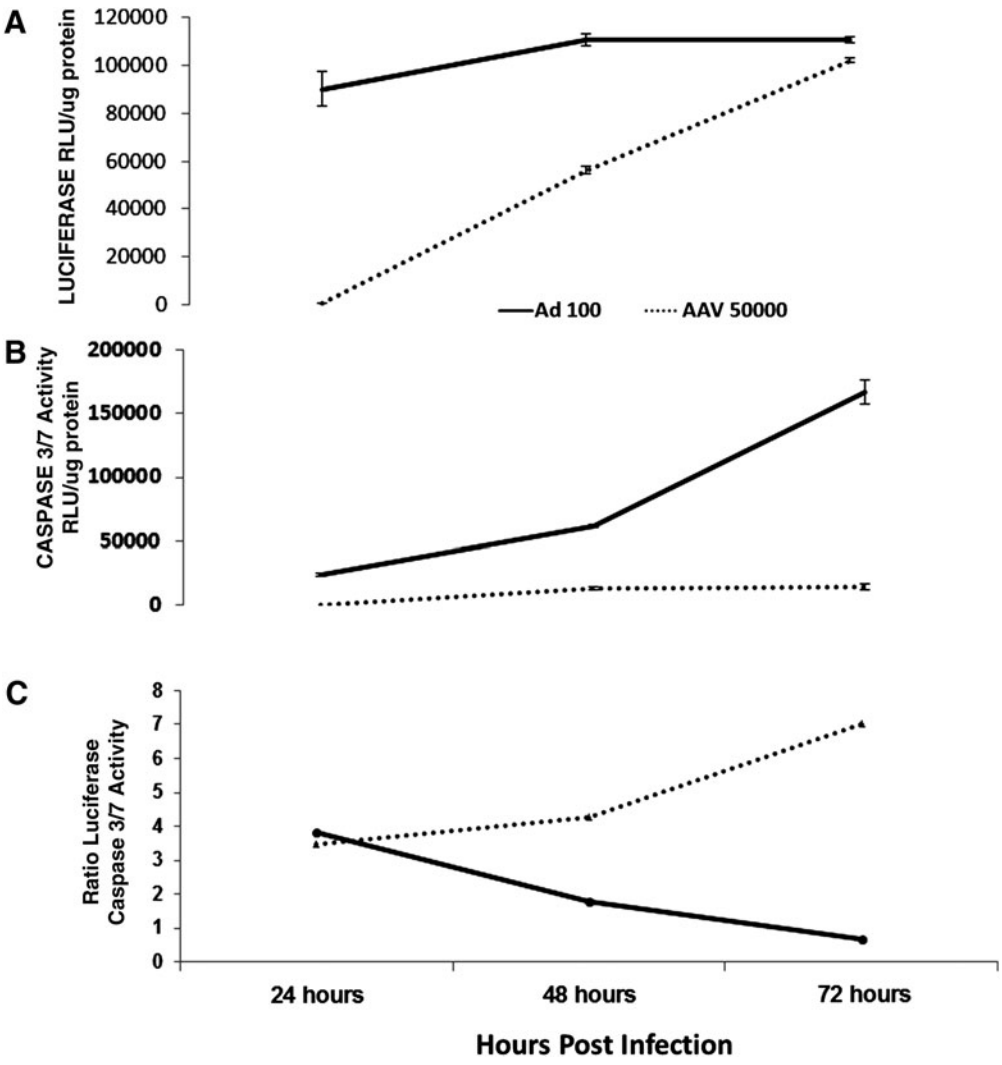

FIG. 5. SASTG vectors exhibit reduced caspase-3/7 activation compared with adenoviral vectors in RNNCs. RNNCs were infected with Ad-luciferase (100 particles per cell) or SASTG-luciferase (50,000 particles per cell). At 24, 48, and 72 hr postinfection, equivalent protein amounts were used to assess luciferase activity **(A)**, using the Promega luciferase assay reagent, or **(B)** caspase-3/7 activity, using the Promega Caspase-Glo 3/7 assay system. Both assays were analyzed with a Veritas luminometer from Turner Biosystems. **(C)** The ratio of vector-expressed luciferase to caspase-3/7 activity is shown. Each time point was examined in triplicate. Data represent means ± SD.

present, limited numbers of drug-based therapies exist for early-stage heart failure, and although these therapies limit progression of heart failure, they do not prevent onset after cardiac injury and these drugs often have adverse side effects (e.g., hypotension). Furthermore, treatments for end-stage heart failure including mechanical assist devices (e.g., a left ventricular assist device [LVA]D) and orthotopic heart transplantation are limited by high cost, bleeding, infection, and/or donor supply. New and improved treatment strategies are needed, and gene therapy is envisioned as one of the

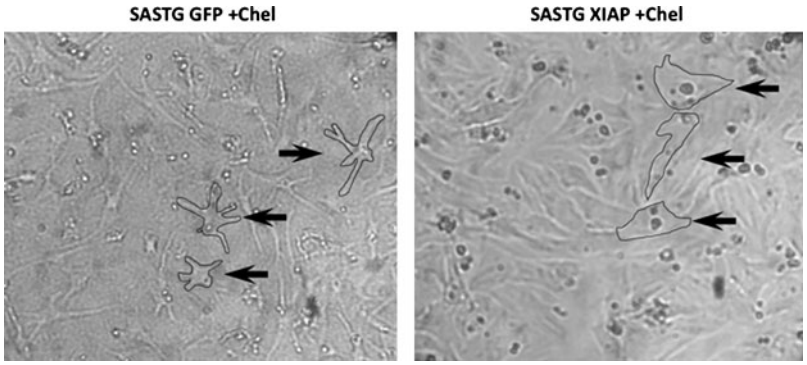

FIG. 6. SASTG-mediated delivery of XIAP ameliorates apoptosis in RNNCs. Shown are photographs of RNNCs treated with chelerythrine 72 hr posttreatment with SASTG-XIAP (*right*) or SASTG-GFP (*left*). The cell membrane is outlined in selected cells (arrows) to emphasize the attenuation of cytoplasm and to pinpoint nuclei in RNNCs exposed to chelerythrine without SASTG-XIAP transduction, suggestive of activation of apoptosis.

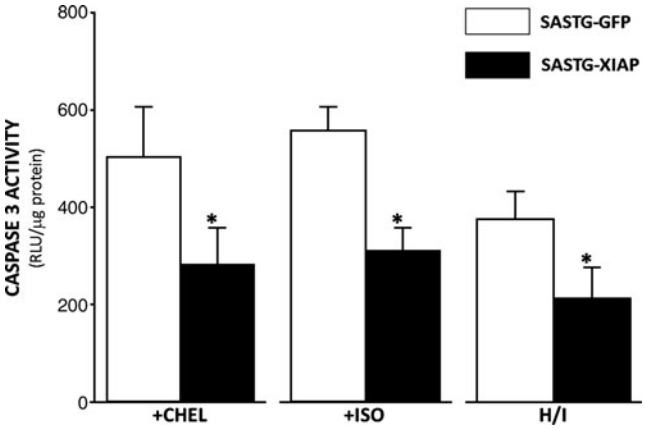

FIG. 7. Pretreatment of RNNCs with SASTG-XIAP vector diminishes caspase-3/7 activation after exposure to three types of apoptotic inducers. RNNCs (10,000 cells per well) were transduced with SASTG-GFP or SASTG-XIAP (20,000 particles/cell). Treatments to induce apoptosis (chelerythrine [CHEL], isoproterenol [ISO], hypoxia–ischemia [H/I]) were performed on cells approximately 72 hr posttransduction in triplicate. CHEL was added to the medium for 1 hr at a final concentration of 1 μM. ISO (1 μM) was added to the medium for 24 hr. H/I was induced by placing cells in an airtight container at 37°C and altering the O_2 concentration over a 24-hr period. Cells from all experiments were lysed and assayed for caspase-3/7 activity, and normalized to total protein. $^*p < 0.05$.

most promising therapeutic options for heart failure. According to Kratlian and Hajjar, three main factors are necessary for successful gene therapy: (1) a molecular target appropriate for the disease, (2) successful vector design, and (3) targeted delivery methods (Kratlian and Hajjar, 2012). Here we describe a new molecular target, the X-linked inhibitor of apoptosis protein (XIAP), for cardiac gene therapy as well as optimization of the AAV capsid design for enhanced cardiac gene delivery.

We first demonstrate that the molecular target XIAP, a potent inhibitor of apoptosis, is reduced in failing human hearts, compared with nonfailing human hearts (Fig. 1). Previous reports have been inconsistent in demonstrating changes in myocardial XIAP levels in failing versus nonfailing human samples (Scheubel *et al.*, 2002; Haider *et al.*, 2009). In our study, XIAP levels were detected and quantitated by two independent methods. Care was taken to standardize tissue procurement and storage, and nonfailing control samples were matched for age and sex. We show definitively that XIAP levels are diminished in human heart failure. Correspondingly, the activity of a late marker of apoptosis, caspase-3/7, was increased in failing human hearts. The most important proapoptotic enzymes, caspases 3, 8, and 9, were previously demonstrated to progressively increase in activity during the transition from preserved LV function to heart failure in porcine myocardium (Moorjani *et al.*, 2009). Perhaps the most convincing evidence for the involvement of apoptosis in heart failure originates from a study examining the number of apoptotic nuclei in transgenic mice expressing a conditionally active form of caspase-8 specifically in the myocardium, wherein a low apoptotic index of 0.23 was sufficient to cause lethal dilated cardiomyopathy (Wencker *et al.*, 2003). Other cardiac stresses that appear to be early triggers for increased apoptosis in the myocardium include increases in LV pressure and volume overload (Cheng *et al.*, 1995; Abbate *et al.*, 2003; Yankey *et al.*, 2008). Furthermore, β-adrenergic antagonists and angiotensin-converting enzyme inhibitors, the most important clinical medications for early heart failure, have been shown to reduce myocardial apoptosis (Kajstura *et al.*, 1997; Romeo *et al.*, 2000; Rossig *et al.*, 2000).

Therefore, methods to inhibit the activities of proapoptotic caspases are promising therapeutic options in the treatment of heart failure. A clear understanding of the amounts, activities, and regulation of inhibitors of proapoptotic proteins in the human heart and heart failure models are crucial to the development of antiapoptotic gene therapy treatments for heart failure. Because XIAP is a potent inhibitor of proapoptotic caspases that is diminished during heart failure, a logical therapeutic approach would be to augment XIAP expression through *in vivo* delivery to cardiomyocytes. AAV-derived vectors are increasingly receiving U.S. Food and Drug Administration (FDA) approval for therapeutic gene delivery in a number of clinical trials (Mingozzi and High, 2011). The success of these vectors in clinical trials was emphasized at a national meeting (Kaiser, 2011). The rational design of AAV2 into a vector, AAV2.5, with enhanced skeletal muscle transduction was used in a clinical trial for muscular dystrophy (Bowles *et al.*, 2011). The rationale for the development of AAV2.5 was derived from amino acid alignments of capsids from serotypes that transduce skeletal muscle with high efficiency (AAV1, AAV7, AAV8, AAV9), compared with those that are inefficient (AAV2, AAV3b) (Xiao *et al.*, 1999; Chao *et al.*, 2000, 2001; Louboutin *et al.*, 2005; Wu *et al.*, 2006). These alignments, together with the atomic structure of the AAV2 capsid, revealed five amino acid sites in AAV2 that were genetically modified via replacement or insertion of the corresponding amino acids from AAV1, yielding AAV2.5. In the current study we have narrowed this region, demonstrating that a single amino acid insertion, T265, in the AAV2 capsid is sufficient to enhance skeletal muscle transduction to a level similar to AAV2.5 (Fig. 2B). Notably, the enhanced transduction profile observed by transfer of these particular amino acids was not restricted to the AAV2 capsid, as demonstrated by enhanced skeletal muscle transduction of the SASTG vector derived from AAV3b (Fig. 2C and D). Apparently, the Q263A/T265 modifications comprise a portable system that can modulate the transduction properties of at least AAV2 and AAV3b, possibly extending to other AAVs. These data indicate that the Q263A/T265 modifications may alter the capsid structural properties of AAV2 and AAV3b at the 2-fold axis of symmetry during the transduction process. Most importantly, however, the SASTG vector dramatically exceeded the transduction efficiency of AAV1, AAV9, and subvariants of AAV2 during *in vivo* transduction of the heart (Fig. 3). Moreover, SASTG was most efficient at transducing primary neonatal rat cardiomyocytes when evaluated against a panel of conventional AAV vectors (Fig. 4). The high efficiency of heart and cardiomyocyte transduction makes SASTG a promising candidate for delivery of therapeutic transgenes to cardiac tissue.

By employing the attributes of SASTG, we may be able to deliver antiapoptotic proteins, such as XIAP, to abate the

effects of apoptosis in diseased hearts. Therefore, a vector offering minimal apoptosis induction would be advantageous. We compared transgene expression and caspase-3/7 activation after transduction with either SASTG or an adenoviral vector. Adenoviral vectors can be toxic to cardiac myocytes, and part of the toxicity might be due to apoptosis induction. Certain cardiomyopathies are in fact associated with adenoviral infections (Savon *et al.*, 2008). We show comparatively that SASTG vectors induced significantly less activation of the caspase cascade relative to adenoviral vectors while at the same time retaining high levels of transgene expression (Fig. 5). These data suggest that in the absence of any other stimuli, adenoviral vectors activated the apoptotic cascade in cultured neonatal cardiac myocytes. Accordingly, the SASTG vector offers the greatest transgene expression with the least induction of apoptosis. This finding is consistent with those of Stilwell and colleagues, who have demonstrated that AAV vectors minimally perturb cellular gene transcription when compared with adenoviral vectors (Stilwell *et al.*, 2003; Stilwell and Samulski, 2004). On the basis of the attributes of SASTG, this vector was employed to deliver XIAP to primary rat neonatal cardiomyocytes. Cardiomyocytes expressing XIAP were significantly protected from apoptosis induced by three different cardiac stresses (Figs. 6 and 7).

Here we provide the initial proof-of-principle experiments that lay the groundwork to use XIAP as a possible therapy for ischemia–reperfusion injury and the deleterious remodeling that can lead to heart failure. Furthermore, we report the development of the SASTG AAV vector, which exhibits a highly efficient cardiac transduction profile with minimal activation of the apoptotic cascade. Coupled with the minimal activation of caspase-3/7, SASTG-XIAP appears to be an efficient vector for attenuation of apoptosis in cardiac myocytes. Our future work will comprise animal studies to derive the true translational value of SASTG-XIAP for potential heart failure therapy.

Acknowledgments

This work was funded by grants NIH 5R01HL072183-03 and 5P01HL075443-04900, and by the W. Gerald Austen Young Investigator Award Society of Thoracic Surgeons (STS), to Dr. Milano; by NIH HL-083342 to Dr. Bursac; by 0630218N from the American Heart Association to Dr. Bowles; by NHLBI P01 HL066973 and NINDS R01 AI072176 to Dr. Samulski; and by RSG-08-290-01-CCE from the American Cancer Society to Dr. Devi.

Author Disclosure Statement

R.J.S. and D.E.B. declare that they are coinventors on a related patent, and in future may receive financial compensation through commercialization of this technology.

References

Abbate, A., Biondi-Zoccai, G.G., Bussani, R., *et al.* (2003). Increased myocardial apoptosis in patients with unfavorable left ventricular remodeling and early symptomatic post-infarction heart failure. J. Am. Coll. Cardiol. 41, 753–760.

Bish, L.T., Morine, K., Sleeper, M.M., *et al.* (2008a). Adeno-associated virus (AAV) serotype 9 provides global cardiac gene transfer superior to AAV1, AAV6, AAV7, and AAV8 in the mouse and rat. Hum. Gene Ther. 19, 1359–1368.

Bish, L.T., Sleeper, M.M., Brainard, B., *et al.* (2008b). Percutaneous transendocardial delivery of self-complementary adeno-associated virus 6 achieves global cardiac gene transfer in canines. Mol. Ther. 16, 1953–1959.

Bowles, D.E., McPhee, S.W.J., Li, C., *et al.* (2011). Phase 1 gene therapy for Duchenne muscular dystrophy using a designer AAV vector. Mol. Ther. 20, 443–455.

Chao, H., Liu, Y., Rabinowitz, J., *et al.* (2000). Several log increase in therapeutic transgene delivery by distinct adeno-associated viral serotype vectors. Mol. Ther. 2, 619–623.

Chao, H., Monahan, P.E., Liu, Y., *et al.* (2001). Sustained and complete phenotype correction of hemophilia B mice following intramuscular injection of AAV1 serotype vectors. Mol. Ther. 4, 217–222.

Chatterjee, S., Stewart, A.S., Bish, L.T., *et al.* (2002). Viral gene transfer of the antiapoptotic factor Bcl-2 protects against chronic postischemic heart failure. Circulation 106, I212–217.

Cheng, W., Li, B., Kajstura, J., *et al.* (1995). Stretch-induced programmed myocyte cell death. J. Clin. Invest. 96, 2247–2259.

Czerski, L., and Nunez, G. (2004). Apoptosome formation and caspase activation: Is it different in the heart? J. Mol. Cell. Cardiol. 37, 643–652.

Du, L., Kido, M., Lee, D.V., *et al.* (2004). Differential myocardial gene delivery by recombinant serotype-specific adeno-associated viral vectors. Mol. Ther. 10, 604–608.

Gao, G., Bish, L.T., Sleeper, M.M., *et al.* (2011). Transendocardial delivery of AAV6 results in highly efficient and global cardiac gene transfer in rhesus macaques. Hum. Gene Ther. 22, 979–984.

Grieger, J.C., Choi, V.W., and Samulski, R.J. (2006). Production and characterization of adeno-associated viral vectors. Nat. Protoc. 1, 1412–1428.

Gustafsson, A.B., and Gottlieb, R.A. (2008). Heart mitochondria: Gates of life and death. Cardiovasc. Res. 77, 334–343.

Gwathmey, J.K., Yerevanian, A.I., and Hajjar, R.J. (2011). Cardiac gene therapy with SERCA2a: From bench to bedside. J. Mol. Cell. Cardiol. 50, 803–812.

Haider, N., Arbustini, E., Gupta, S., *et al.* (2009). Concurrent upregulation of endogenous proapoptotic and antiapoptotic factors in failing human hearts. Nat. Clin. Pract. Cardiovasc. Med. 6, 250–261.

Hajjar, R.J., Zsebo, K., Deckelbaum, L., *et al.* (2008). Design of a phase 1/2 trial of intracoronary administration of AAV1/SERCA2a in patients with heart failure. J. Card. Fail. 14, 355–367.

Jaski, B.E., Jessup, M.L., Mancini, D.M., *et al.* (2009). Calcium upregulation by percutaneous administration of gene therapy in cardiac disease (CUPID Trial), a first-in-human phase 1/2 clinical trial. J. Card. Fail. 15, 171–181.

Kaiser, J. (2011). Gene therapists celebrate a decade of progress. Science 334, 29–30.

Kajstura, J., Cigola, E., Malhotra, A., *et al.* (1997). Angiotensin II induces apoptosis of adult ventricular myocytes *in vitro*. J. Mol. Cell. Cardiol. 29, 859–870.

Kawamoto, S., Shi, Q., Nitta, Y., *et al.* (2005). Widespread and early myocardial gene expression by adeno-associated virus vector type 6 with a β-actin hybrid promoter. Mol. Ther. 11, 980–985.

Khoynezhad, A., Jalali, Z., and Tortolani, A.J. (2007). A synopsis of research in cardiac apoptosis and its application to congestive heart failure. Tex. Heart Inst. J. 34, 352–359.

Kratlian, R.G., and Hajjar, R.J. (2012). Cardiac gene therapy: From concept to reality. Curr. Heart Fail. Rep. 9, 33–39.

Laugwitz, K.L., Moretti, A., Weig, H.J., *et al.* (2001). Blocking caspase-activated apoptosis improves contractility in failing myocardium. Hum. Gene Ther. 12, 2051–2063.

Louboutin, J.P., Wang, L., and Wilson, J.M. (2005). Gene transfer into skeletal muscle using novel AAV serotypes. J. Gene Med. 7, 442–451.

Masri, C., and Chandrashekhar, Y. (2008). Apoptosis: A potentially reversible, meta-stable state of the heart. Heart Fail. Rev. 13, 175–179.

Mingozzi, F., and High, K.A. (2011). Therapeutic *in vivo* gene transfer for genetic disease using AAV: Progress and challenges. Nat. Rev. Genet. 12, 341–355.

Moorjani, N., Westaby, S., Narula, J., *et al.* (2009). Effects of left ventricular volume overload on mitochondrial and death-receptor-mediated apoptotic pathways in the transition to heart failure. Am. J. Cardiol. 103, 1261–1268.

Okada, H., Takemura, G., Kosai, K., *et al.* (2005). Postinfarction gene therapy against transforming growth factor-β signal modulates infarct tissue dynamics and attenuates left ventricular remodeling and heart failure. Circulation 111, 2430–2437.

Okada, H., Takemura, G., Kosai, K., *et al.* (2009). Combined therapy with cardioprotective cytokine administration and antiapoptotic gene transfer in postinfarction heart failure. Am J. Physiol. Heart Circ. Physiol. 296, H616–H626.

O'Riordan, M.X., Bauler, L.D., Scott, F.L., and Duckett, C.S. (2008). Inhibitor of apoptosis proteins in eukaryotic evolution and development: A model of thematic conservation. Dev. Cell 15, 497–508.

Pacak, C.A., and Byrne, B.J. (2011). AAV vectors for cardiac gene transfer: Experimental tools and clinical opportunities. Mol. Ther. 19, 1582–1590.

Pacak, C.A., Mah, C.S., Thattaliyath, B.D., Conlon, T.J., *et al.* (2006). Recombinant adeno-associated virus serotype 9 leads to preferential cardiac transduction *in vivo*. Circ. Res. 99, e3–e9.

Palomeque, J., Chemaly, E.R., Colosi, P., *et al.* (2007). Efficiency of eight different AAV serotypes in transducing rat myocardium *in vivo*. Gene Ther. 14, 989–997.

Pedrotty, D.M., Klinger, R.Y., Kirkton, R.D., and Bursac, N. (2009). Cardiac fibroblast paracrine factors alter impulse conduction and ion channel expression of neonatal rat cardiomyocytes. Cardiovasc. Res. 83, 688–697.

Pulicherla, N., Shen, S., Yadav, S., *et al.* (2011). Engineering liver-detargeted AAV9 vectors for cardiac and musculoskeletal gene transfer. Mol. Ther. 19, 1070–1078.

Rabinowitz, J.E., Rolling, F., Li, C., *et al.* (2002). Cross-packaging of a single adeno-associated virus (AAV) type 2 vector genome into multiple AAV serotypes enables transduction with broad specificity. J. Virol. 76, 791–801.

Regula, K.M., and Kirshenbaum, L.A. (2005). Apoptosis of ventricular myocytes: A means to an end. J. Mol. Cell. Cardiol. 38, 3–13.

Roger, V.L., Go, A.S., Lloyd-Jones, D.M., *et al.* (2012a). Executive summary: Heart disease and stroke statistics—2012 update: A report from the American Heart Association. Circulation 125, 188–197.

Roger, V.L., Go, A.S., Lloyd-Jones, D.M., *et al.* (2012b). Heart disease and stroke statistics—2012 update: A report from the American Heart Association. Circulation 125, e2–e220.

Romeo, F., Li, D., Shi, M., and Mehta, J.L. (2000). Carvedilol prevents epinephrine-induced apoptosis in human coronary artery endothelial cells: Modulation of Fas/Fas ligand and caspase-3 pathway. Cardiovasc. Res. 45, 788–794.

Rossig, L., Haendeler, J., Mallat, Z., *et al.* (2000). Congestive heart failure induces endothelial cell apoptosis: Protective role of carvedilol. J. Am. Coll. Cardiol. 36, 2081–2089.

Savon, C., Acosta, B., Valdes, O., *et al.* (2008). A myocarditis outbreak with fatal cases associated with adenovirus subgenera C among children from Havana City in 2005. J. Clin. Virol. 43, 152–157.

Scheubel, R.J., Bartling, B., Simm, A., *et al.* (2002). Apoptotic pathway activation from mitochondria and death receptors without caspase-3 cleavage in failing human myocardium: Fragile balance of myocyte survival? J. Am. Coll. Cardiol. 39, 481–488.

Stilwell, J.L., and Samulski, R.J. (2004). Role of viral vectors and virion shells in cellular gene expression. Mol. Ther. 9, 337–346.

Stilwell, J.L., McCarty, D.M., Negishi, A., *et al.* (2003). Development and characterization of novel empty adenovirus capsids and their impact on cellular gene expression. J. Virol. 77, 12881–12885.

Su, H., Huang, Y., Takagawa, J., *et al.* (2006). AAV serotype-1 mediates early onset of gene expression in mouse hearts and results in better therapeutic effect. Gene Ther. 13, 1495–1502.

Su, H., Yeghiazarians, Y., Lee, A., *et al.* (2008). AAV serotype 1 mediates more efficient gene transfer to pig myocardium than AAV serotype 2 and plasmid. J. Gene Med. 10, 33–41.

Tarantal, A.F., and Lee, C.C. (2009). Long-term luciferase expression monitored by bioluminescence imaging after adeno-associated virus-mediated fetal gene delivery in rhesus monkeys (*Macaca mulatta*). Hum. Gene Ther. 21, 143–148.

Wang, Z., Zhu, T., Qiao, C., *et al.* (2005). Adeno-associated virus serotype 8 efficiently delivers genes to muscle and heart. Nat. Biotechnol. 23, 321–328.

Wasala, N.B., Shin, J.H., and Duan, D. (2011). The evolution of heart gene delivery vectors. J. Gene Med. 13, 557–565.

Wencker, D., Chandra, M., Nguyen, K., *et al.* (2003). A mechanistic role for cardiac myocyte apoptosis in heart failure. J. Clin. Invest. 111, 1497–1504.

Whelan, R.S., Kaplinskiy, V., and Kitsis, R.N. (2010). Cell death in the pathogenesis of heart disease: Mechanisms and significance. Annu. Rev. Physiol. 72, 19–44.

Williams, M.L., and Koch, W.J. (2004). Viral-based myocardial gene therapy approaches to alter cardiac function. Annu. Rev. Physiol. 66, 49–75.

Wu, Z., Asokan, A., and Samulski, R.J. (2006). Adeno-associated virus serotypes: Vector toolkit for human gene therapy. Mol. Ther. 14, 316–327.

Xiao, W., Chirmule, N., Berta, S.C., *et al.* (1999). Gene therapy vectors based on adeno-associated virus type 1. J. Virol. 73, 3994–4003.

Yamamoto, S., Seta, K., Morisco, C., *et al.* (2001). Chelerythrine rapidly induces apoptosis through generation of reactive oxygen species in cardiac myocytes. J. Mol. Cell. Cardiol. 33, 1829–1848.

Yang, L., Jiang, J., Drouin, L.M., *et al.* (2009). A myocardium tropic adeno-associated virus (AAV) evolved by DNA shuffling and *in vivo* selection. Proc. Natl. Acad. Sci. U.S.A. 106, 3946–3951.

Yankey, G.K., Li, T., Kilic, A., *et al.* (2008). Regional remodeling strain and its association with myocardial apoptosis after myocardial infarction in an ovine model. J. Thorac. Cardiovasc. Surg. 135, 991–998, e991–e992.

Zincarelli, C., Soltys, S., Rengo, G., and Rabinowitz, J.E. (2008). Analysis of AAV serotypes 1–9 mediated gene expression and tropism in mice after systemic injection. Mol. Ther. 16, 1073–1080.

Zolotukhin, S., Byrne, B.J., Mason, E., *et al.* (1999). Recombinant adeno-associated virus purification using novel methods improves infectious titer and yield. Gene Ther. 6, 973–985.

Zorc-Pleskovic, R., Alibegovic, A., Zorc, M., *et al.* (2006). Apoptosis of cardiomyocytes in myocarditis. Folia Biol. (Praha) 52, 6–9.

Address correspondence to:
Dr. Dawn E. Bowles
Department of Surgery, Division of Surgical Sciences
Duke University Medical Center, Box 2642
Research Drive
Durham, NC 27710

E-mail: dawn.bowles@duke.edu

Received for publication October 15, 2011;
accepted after revision February 9, 2012.

Published online: February 16, 2012.